Analysis of Thermal Decomposition Kinetics and Calculation of Activation Energy for Degradation of Polyaniline-Graphene Oxide Composites-Synergistic Reinforcement on Thermal Stability

Gul, Hajera
National Centre of Excellence in Physical Chemistry, University of Peshawar, 25120 Peshawar, PAKISTAN

Ali Shah, Anwar-Ul-Haq
Institute of Chemical Sciences, University of Peshawar, 25120 Peshawar, PAKISTAN

Gul, Salma
Department of Chemistry, Women University Swabi, 22102 Swabi, PAKISTAN

Bilal, Slama*[+]
National Centre of Excellence in Physical Chemistry, University of Peshawar, 25120 Peshawar, PAKISTAN

ABSTRACT: *Thermo Gravimetric Analysis (TGA) is one of the most commonly used techniques to study the thermal stability of materials. Thermograms not only give an instant view of thermal stability but can also give insights into the degradation kinetics of the material. This study reports on the degradation kinetics of composite materials based on polyaniline and graphene oxide (PANI-GO) synthesized with varying amounts of GO. Horwitz & Metzger, Coats & Redfern, and Chan et al., methods were employed for the calculation of activation energy for degradation, using TGA data. It was observed that their thermal stability and activation energy of degradation are affected by changing the amount of GO during polymerization, indicating PANI and GO synergistically enhance the thermal stability of PANI-GO composites. The highest activation energy value of 29.87 kJ/mol was shown by a composite that contains 6 percent GO. UltraViolet-Visible (UV-Vis) spectroscopy, X-Ray Diffraction (XRD) Analysis also support variations in different properties of the composites as a result of changing GO concentration.*

KEYWORDS: *Polyaniline-graphene oxide composites; activation energy of degradation; Horwitz & Metzger method; Coats & Redfern methods.*

***** *To whom correspondence should be addressed.*
+ *E-mail*: *salmabilal@uop.edu.pk*
1021-9986/2022/3/875-889 *15/$/6.05*

INTRODUCTION

The thermal stability of intrinsically conducting polymers is an important issue [1]. For many practical applications such as solar cells, supercapacitors, and batteries, the thermal stability of the material is of prime importance [2]. ThermoGravimetric Analysis (TGA) is an important technique for measuring weight loss and its rate of change with respect to temperature/time in a controlled atmosphere. TGA studies are generally used for finding the thermal stability of materials.

While performing TGA, a linear heating program is applied [3]. At a certain heating rate, the temperature rises from a lower to a defined higher value. Thus, in a single experiment thermal behavior of the sample at different temperatures can be monitored. During the experiment, the mass of the sample is recorded continuously in a controlled atmosphere. The thermal behavior of the sample can be predicted from the recorded mass loss curve. These curves can be utilized for the determination of activation energy with the help of various integral methods [4].

Modern TGA equipment generally records hundreds or thousands of experimental points that can be used for kinetic analysis of the reaction [5]. While analyzing the data, the selection of the correct model is one of the important factors. Researchers have conducted detailed studies to know how experimental data can be justified by a model. Several researchers have developed different methodologies
to study degradation kinetics, among them *Horowitz-Metzger*, *Coats-Redfern*, and *Chan et al.*, methods are most commonly used [6].

Polymers and polymer composites are of great importance for various applications and detailed knowledge of their thermal decomposition behavior is necessary. Among conducting polymers, polyaniline (PANI) is important due to its low cost, easy preparation procedures [7], and excellent thermal, environmental and electrochemical stability [8]. In this research, we present a thorough analysis of the thermal degradation kinetics of PANI and its composites with graphene oxide (PANI-GO) using *Horowitz-Metzger*, *Coats-Redfern*, and *Chan et al.*, methods. It is an established fact that the properties of PANI-based materials greatly vary with varying experimental conditions such as the method of synthesis and sample composition, etc., employed during synthesis. Here, we have shown how the different physicochemical and structural properties are affected by changing sample composition with special emphasis on thermal degradation behavior. Generally, the degradation process of PANI and its composites takes place in two or three steps [9]. These steps can be assigned to the elimination of water, loss of dopants, and finally breakdown of the polymer backbone. The thermogravimetric data was utilized to calculate the activation energy of degradation of the synthesized materials. To the best of the author's knowledge, no detailed study is available to find out the activation energy of degradation for PANI-GO composites.

EXPERIMENTAL SECTION

Materials

Aniline ($C_6H_5NH_2$), Sigma-Aldrich (Hamburg, Germany), was double distilled under reduced pressure and stored in a refrigerator. Chloroform ($CHCl_3$), sulfuric acid (H_2SO_4), and hydrochloric acid (HCl) were purchased from Scharlau Chemie S.A (08181 Sentmenat, Spain) and used as received. Dodecylbenzenesulfonic acid, DBSA, ($C_{12}H_{25}C_6H_4SO_3H$), ammonium persulfate, APS, ($(NH_4)_2S_2O_8$)), graphite powder, potassium permanganate ($KMnO_4$), sodium nitrate ($NaNO_3$), hydrogen peroxide (H_2O_2) dimethylformamide (DMF), polytetrafluoroethylene (PTFE) and acetone were purchased from Sigma-Aldrich (Hamburg, Germany). All these chemicals were research-grade and used without further purification.

Synthesis of Graphene Oxide Sheets

The graphene oxide (GO) was manufactured by the Modified Hummer's method [1]. 2.0 g of graphite powder was dispersed in 46 mL of H_2SO_4 for 2 hours. H_2SO_4 act as intercalated molecules to facilitate the oxidation of bulk graphite. 6 g of $KMnO_4$ and 1 g of $NaNO_3$ were added to it while stirring. $KMnO_4$ along with H_2SO_4 enhances oxidation while $NaNO_3$ supports oxidation at the basal plane of graphite. The temperature was maintained at less than 20 ºC. This mixture was then stirred at 35 ºC for 30 minutes. Then 92 mL of deionized water was gradually added to the above suspension, which resulted in violent effervescence. The temperature of the reaction mixture was maintained at 98 ºC for 15 minutes. Afterward, 280 mL of deionized water was added to the obtained suspension, in order to dilute it. This was followed by treatment with 30% H_2O_2 (10 mL) to remove unreacted permanganate.

The subsequent suspension was washed with 5% HCl aqueous solution and an excess amount of deionized water to eliminate salt residues. The GO thus produced was sonicated to produce persistent GO dispersion in water (Fig. S1)

Synthesis of PANI-GO Composites

First GO (0.015 g) was dispersed in distilled water (20 mL) through sonication. Sonication was carried out for 30 minutes to form homogeneous dispersion [10]. In another step, 2.3 mL of dodecylbenzenesulfonic acid (DBSA) was added to 50 mL of chloroform to a round bottom flask under constant stirring followed by 1.5 mL of aniline to the above reaction mixture. After this 25 mL of 1.1 M of H_2SO_4 and 25 mL of 0.09 M ammonium persulfate (APS) were added dropwise to the stirring reaction mixture. GO dispersion was then added slowly to the above reaction mixture and the reaction was allowed to run for 24 hours under constant stirring. After 24 hours the reaction was stopped and the green color PANI-GO precipitate was washed with distilled water 3 times and then with acetone to remove unreacted species. The PANI-GO precipitate was filtered and dried in an oven at 60 ºC (Fig. S2). Reaction conditions were optimized by varying different reaction parameters such as acid, monomer, oxidant, and GO. Codes assigned to samples based on GO concentration are depicted in Table 1.

Characterizations

The percent yield of composites was calculated on the basis of Equation (1):

$$\text{Percent yield} = \frac{\text{Weight of composite}}{\text{Weight of aniline}} \times 100 \qquad (1)$$

PANI-GO composites were dispersed in chloroform and Ultraviolet-Visible (UV-Vis) spectra were registered with the help of a Perkin Elmer spectrophotometer (Buckinghamshire, UK) using a quartz cell of 1cm path length.

X-Ray Diffraction (XRD) patterns of samples were recorded utilizing Cu Kα radiations (λ = 1.5405 Å) on a Rigaku (JEOL, Tokyo, Japan) X-ray diffractometer with a progressive scan rate of 0.05°/s.

To check the electrochemical response of the material, Electrochemical Impedance Spectroscopy (EIS) of the synthesized materials was carried out in a three-electrode cell, containing 1 M $HClO_4$, using Reference 3000 ZRA potentiostat/galvanostat (Gamry, Warminster, PA, USA). A coiled wire of gold and saturated calomel electrode (SCE) was used as a counter electrode and a reference electrode, respectively. 80% PANI-GO composite, 10% activated carbon, and 10% polytetrafluoroethylene (PTFE) were dispersed in dimethylformamide (DMF). It was deposited in the form of a uniform slurry on a gold sheet electrode, vacuum dried, and used as the working electrode.

Table 1: Sample codes on the bases of GO concentration.

S. No	Sample code	GO concentration (%)
1	PANI-GO-1	1
2	PANI-GO-2	2
3	PANI-GO-4	4
4	PANI-GO-6	6
5	PANI-GO-8	8
6	PANI-GO-10	10
7	PANI	0

The test samples for electrical conductivity were prepared in a pellet form at a pressure of 80 MPa. Four probe methods were used to measure the electrical conductivity of samples by utilizing a RM3000 four-probe resistivity/square resistance tester (Bridge Technology Co.Ltd., Chandler Heights Arizona, USA)

To check the thermal degradation pattern, structural aspects, and thermal stability of composites Thermo Gravimetric Analysis (TGA) was carried out. It was executed by making use of Perkin Elmer (Waltham, MA, USA) at a heating rate 10°/min in the under N_2 atmosphere. TGA data were used to calculate the pre-exponential factor, activation energy, order, and mechanism of a reaction. Horowitz and Metzger method and Coats and Redfern Method were used for these calculations.

RESULTS AND DISCUSSION

Polymerization Mechanism

The mechanism of synthesis of PANI on the surface of GO sheets is depicted in Schemes 1 (a), 1 (b), and 1 (c). Addition of GO to ammonium persulfate (APS), acid and aniline suspension results in the *in-situ* oxidative polymerization of PANI-GO composites [11]

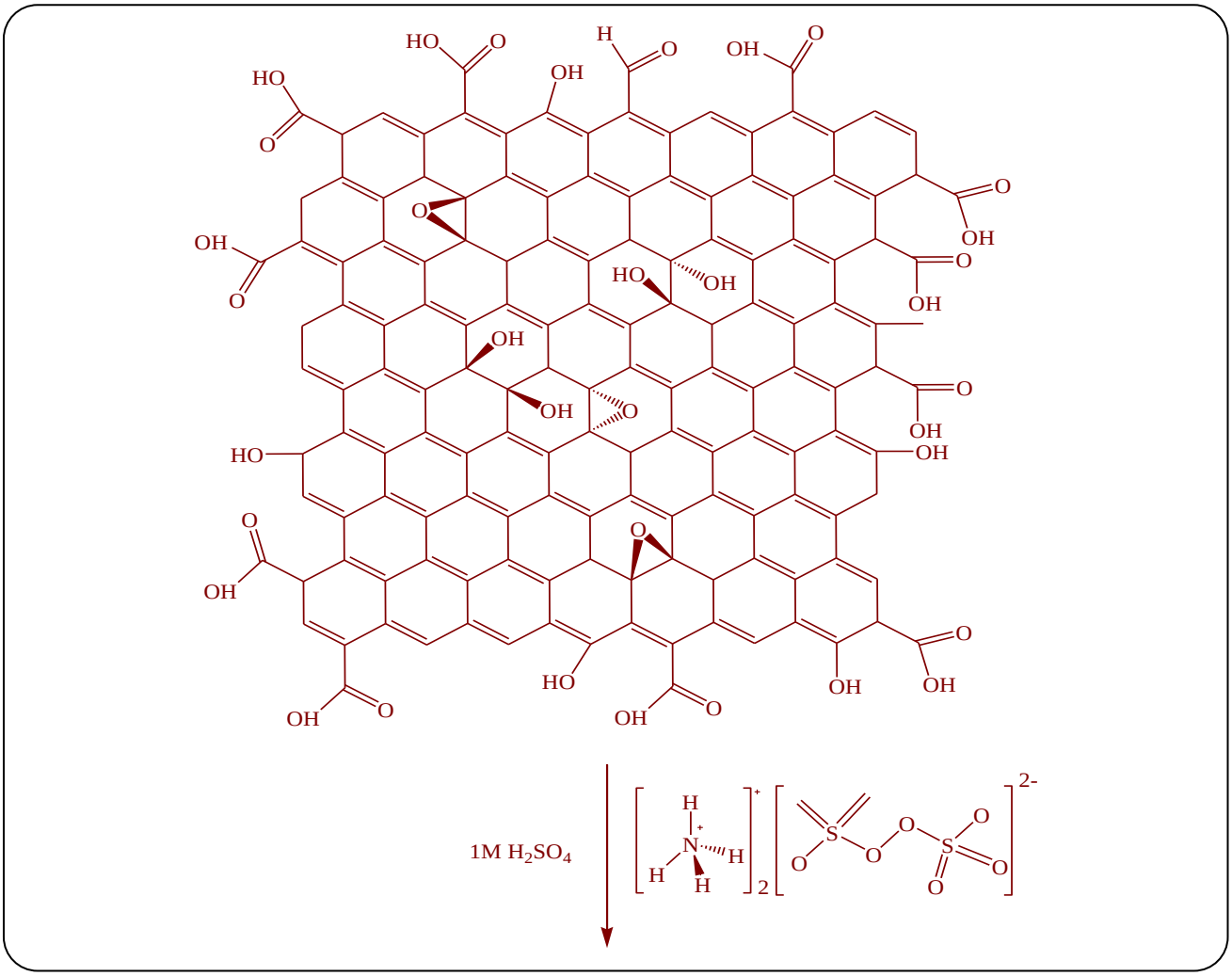

Scheme 1 (a): Initiation of in-situ oxidative chemical polymerization.

It is presumed that APS aqueous solution is attached to the surface of GO sheets as a consequence of electrostatic associations and hydrogen bonds and enhances the polymerization of aniline monomers.

In this synthesis protocol, the APS act not merely as an oxidant for the process of oxidative polymerization of aniline but it also behaves like a surface directing specie to improve the synthesis of PANI on the surface of GO sheets. In the next step, the PANI backbones are additionally stabilized on the surface of GO via Vander Waals forces and π-π interactions [12].

Optimization of Reaction Parameters

Different PANI-GO composites were synthesized by varying different reaction parameters such as the amount of oxidant, acid, monomer, and Graphene Oxide (GO) in order to choose the best conditions. The results are discussed below:

Impact of Oxidant Amount on Percent Yield of PANI-GO Composites

The impact of oxidant amount on yield (%) of PANI-GO composites is illustrated in Fig. S3 (a). Its amount was varied step-wise. Below 0.75 mmol of the oxidant, no product was formed. Percent yield increased with an increase in the amount of oxidant. The maximum percent yield was obtained at 1.75 mmol. Above this value, the percent yield was decreased again. It can be assumed that when a small amount was used, no radical cation formation took place, and thus no product was obtained. As the amount of APS was increased more radical cations were formed leading to a higher amount of polymer [13]. The reason for the decrease

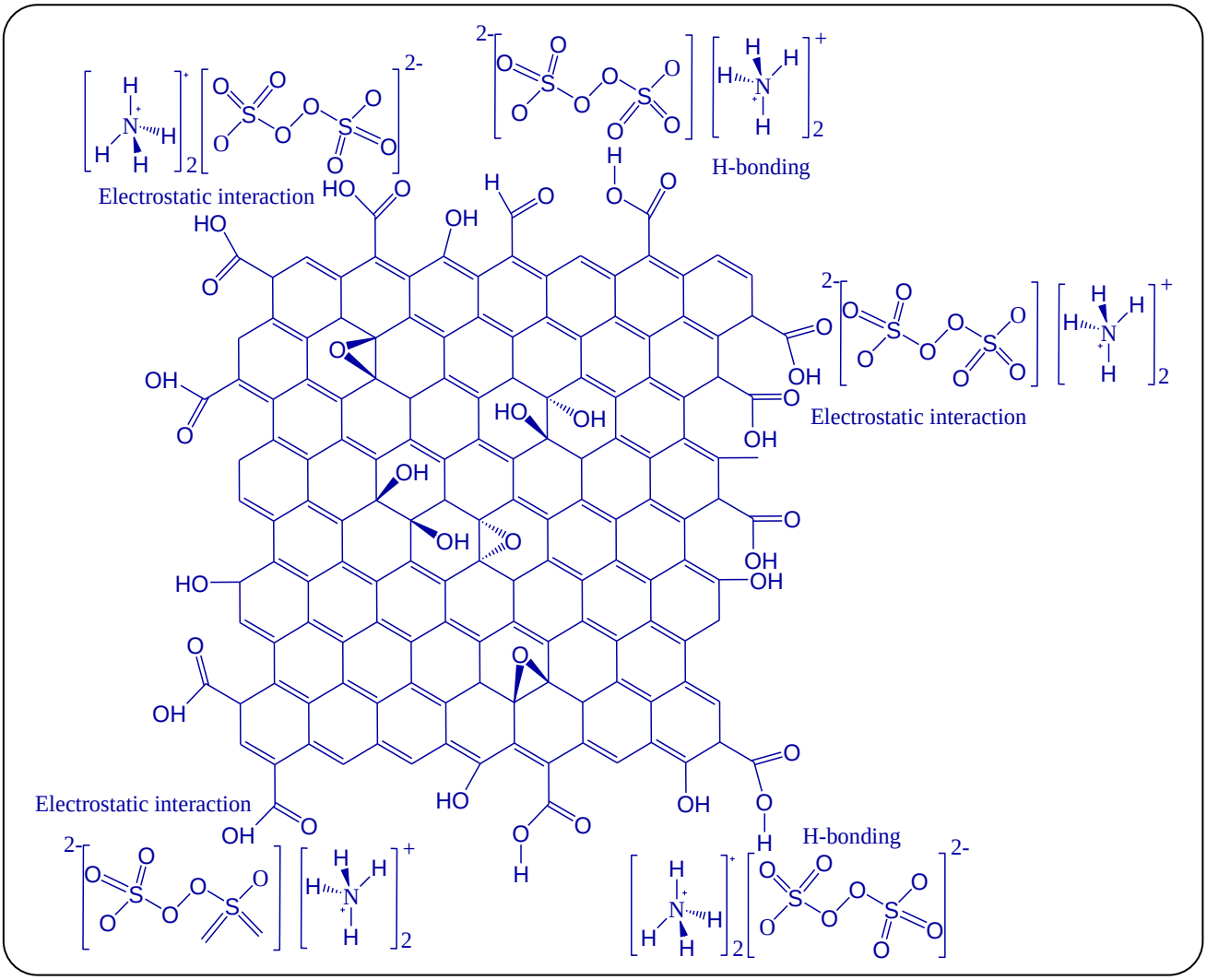

Scheme 1 (b): Interaction of ammonium persulfate with GO.

in the yield of PANI-GO composites with further increased APS amount, is probably the over-oxidation of radical cations. The over-oxidation of radical cations, which are responsible for the growth of the polymer chains, can obstruct polymerization and result in a declined yield.

Another reason for this decline in composite yield, when the amount of oxidant was further increased, might be the production of redundant aniline radical cation and soluble oligomers because of rapid polymerization.

Impact of Acid Amount on Percent Yield of PANI-GO Composites

Fig. S3 (b), depicts the impact of acid amount on the percent yield of PANI-GO composites. Below 12.5 mmol no product was formed. As its amount increased, the composite the composite formation was initiated. The percent yield of product was highest at 27.5 mmol and then decrease with further increase in acid amount.

This behavior is characteristic in relation to the effect of the acid amount on the PANI yield [13]. It might be suggested that aniline molecules cause head-to-tail coupling in acidic media. Subsequently, H^+ has to be removed from the framework for the advancement of the product. At 27.5 mmol of the acid, a remarkable quantity of aniline salt is formed in the medium and aniline cannot react as H^+ acceptor. When H^+ is not removed from the cation radical oligomer, this not only stops the growth of the oligomer but also decomposes by hydrolysis. Another cause for the decline in composite yield when the acid amount was high, can be the degradation of the composite created in the reaction medium.

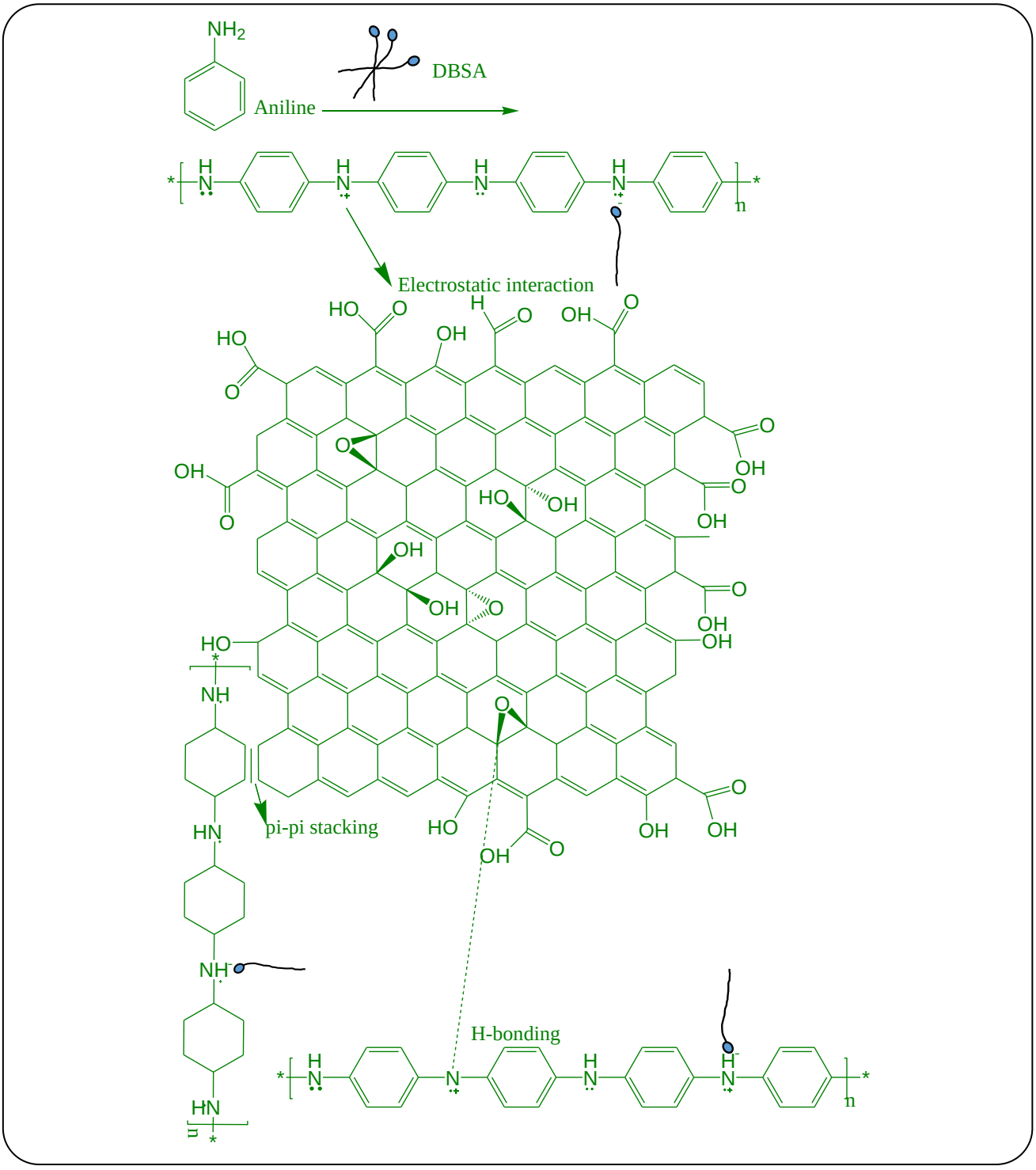

Scheme 1 (c): Formation of PANI-GO composite.

Impact of Monomer Amount on Percent Yield of PANI-GO Composites

The composite yield was increased with an increase in monomer amount and then decreases after 17.42 mmol of aniline (Fig. S3 (c)). This decline in composite yield with a rise in monomer amount may be because of the initiation of an enormous number of monomeric active sites and as a consequence soluble oligomers are formed and thus percent yield is decreased [13].

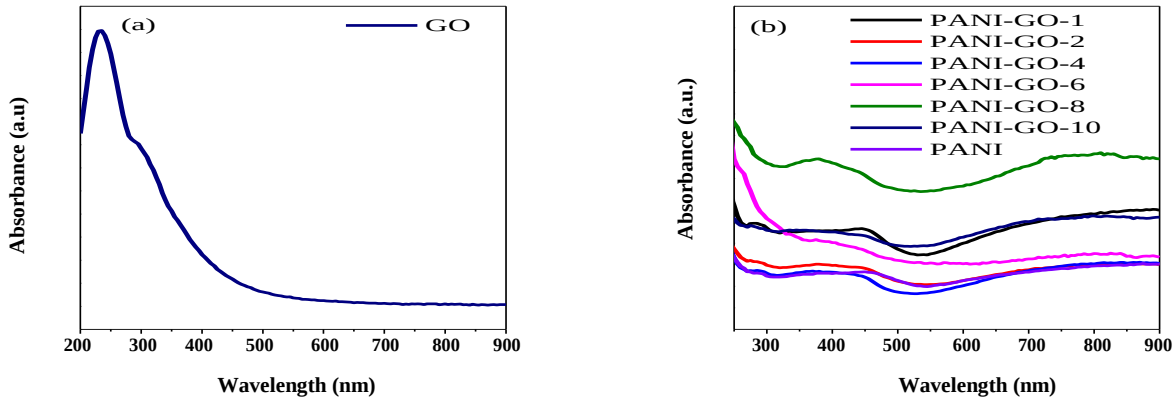

Fig. 1 (a): UV- Visible spectrum of GO; (b): UV-Visible spectra of PANI and PANI-GO composites.

Impact of GO Amount on Percent Yield of PANI-GO Composites

Fig. S3 (d), depicts that composite yield increases with an increase in GO content in the reaction bath. This increase in percent yield might be due to the fact that GO provides active sites for reaction and as its content increases more sites are available for composite formation. The impact of changing GO amount on other properties of the resulting composites was also visible as discussed below.

UV-Visible Spectroscopic Analysis

Fig. 1 (a) and (b) depict the UV-Vis spectra of GO, PANI, and PANI-GO composite. GO was dispersed in distilled water. While PANI and PANI-GO were dispersed in chloroform. The characteristic peak at 233 nm in Fig. 1 (a) is due to of $\pi \rightarrow \pi^*$ shift of C=C while a shoulder at ~290-300 nm, corresponds to $n \rightarrow \pi^*$ transition of C=O bond [14].

In Fig. 1 (b) appearance of the peaks at 287 and 826 nm are illustrative of PANI in its doped form and are ascribed to polaron-π^* and π-polaron transitions, respectively [15]. The absorption peak of π-polaron transition is broader and also emerges at a high wavelength. The blue-shifted band from 826 nm in PANI to 810 nm in PANI-GO might be originated from steric restraint and illustrates the firm attachment of PANI with GO. Due to this interaction between PANI and GO and the formation of π-π bond, the crystallinity of these composites is expected to increase which can ultimately have an effect on the thermal stability

X-Ray Diffraction Analysis

X-Ray Diffraction (XRD) analysis presents immense information about the structural characteristics. Fig. 2 (a) depicts XRD plot of GO. A characteristic peak ($2\theta = 11$), is assigned to the gap of 0.803 nm among layers of GO sheets [14].

The XRD analysis for the PANI and PANI-GO composites is depicted in Fig. 2 (b). In XRD plot, the Bragg diffraction shoulders at 2θ = ~15.07°, 2θ = ~ 20°, and 25.2° appear in PANI salts. These characteristic peaks manifest the emeraldine salt form of PANI, demonstrating that PANI salts have some crystallinity. This crystallinity of PANI might be assigned to the repetition of benzenoid and quinoid units in PANI framework. The centered peak at 2θ = ~20° probably be assigned to recurrence parallel to the polymer chain. A peak positioned at 2θ = ~25.2° might be a result of recurrence perpendicular to the polymer backbone. Also, the peak at 2θ = ~20° illustrates the characteristic distance among the ring planes of benzene in adjoining chains or the nearby inter-chain gap [13]. After incorporation of GO in PANI, the peak at 2θ=11 disappears in PANI-GO composites, showing that GO is completely exfoliated into single graphene oxide sheets. A broad peak appeared at 2θ=25.18º in PANI-GO composites. The XRD pattern of the PANI-GO composites contains reflection peaks parallel in comparison with that of pure PANI, thus depicting prosperous polymerization on the surface of GO [16].

Morphological study

In order to get an idea about the morphology of the synthesized materials, Scanning Electron Microscopy (SEM) was carried out for selected samples (Fig. 3). Fig. 3 (a) showcases SEM image of GO that shows typical flake-like morphology. From Fig. 3 (c) it can be observed that PANI-GO-6 has uniform morphology and a highly porous structure. As GO sheets are densely negatively charged,

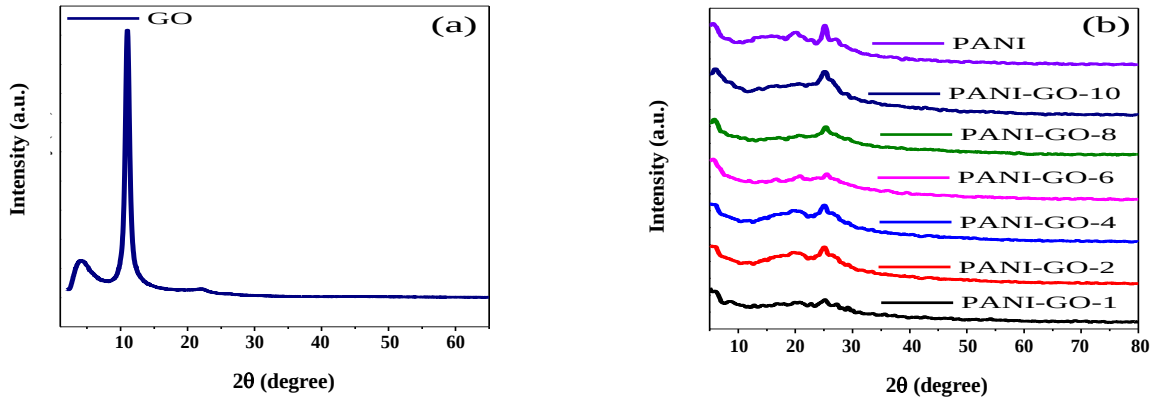

Fig. 2: XRD patterns of (a) GO and (b) PANI and PANI-GO composites.

when dispersed in water, ionization of various oxygen-containing functional groups at the surface of GO sheets takes place [14]. These oxygen-containing functional groups at the surface of GO are active sites for growing PANI-GO composites [17]. Because of the electrostatic and π-π interaction, PANI is uniformly adsorbed at the surface of GO, and thus agglomeration is prevented and can be seen from SEM images in Fig. 3 (c). Due to this prevention of agglomeration PANI-GO-6 has a small particle size that is in the nano range as can be seen from the histogram given in Fig. 3 (d) for PANI-GO-6. To calculate the particle size of PANI-GO-6, Nano Measurer 1.2.5 software was used by converting the pixel values of the SEM images' nm unit. 50 particles were selected and their values are presented in graphical form in Fig. 3 (d). For these particles maximum, minimum, and mean values are 147.75, 30.55, and 66.04 nm.

This interaction between PANI and GO is also confirmed by TGA analysis as PANI-GO-6 show enhanced thermal stability when compared with other composites and PANI. Energy Dispersive X-ray (EDX) analysis in Fig. 3 (e), further supports this morphology as all these elements are present.

Electrochemical activity

The electrochemical activity and internal resistance of the optimized composite were studied through Electrochemical Impedance Spectroscopy (EIS) [15].

Nyquist plot (Fig. S4 (a)) is composed of a depressed semicircle in the high-frequency region and a near-vertical line in the low-frequency region. The small semicircle shows good electrical conductivity and low resistance of the material [18]. Where Rs is the bulk solution resistance and Rct is the charge-transfer resistance [19]. The value of ESR is very small and there is almost no semicircle at the high frequencies also the line at low frequencies is almost vertical. This is because of the porosity of the material and high electrical conductivity which can be seen from SEM images of PANI-GO-6.

Phase angle 82° is close to 90° and thus shows excellent capacitive behavior (Fig. S4 (b)). However, it is diverted from a vertical straight-line in the low-frequency region showing Warburg behavior which is diffusion controlled. It is due to the semi-infinite diffusion of protons at the interface of the composite-electrolyte.

At phase angle 45° particular frequency is known as the knee frequency (f_0).it is the point where the capacitive and the resistive impedances are equivalents [20].

Electrical Conductivity Measurements

The DC electrical conductivity of the PANI-GO composites, in the form of round, pressed pallets, was recorded with the help of the four-probe method by the following equation [21]:

$$\sigma = \frac{1}{\rho} \qquad (2)$$

Where σ and ρ are conductivity [S/cm] and resistivity [Ω cm], respectively. Table 2 shows the conductivity of PANI-GO composites.

The electrical conductivity of PANI was 0.0450 S/cm. The electrical conductivity of its composites with GO was higher than the pristine PANI (Table 2). Mechanism

Table 2: Conductivity measurement of PANI-GO composites.

S.NO	Sample name	Conductivity (S/cm)
1	PANI-GO-1	0.0917
2	PANI-GO-2	0.2222
3	PANI-GO-4	0.3125
4	PANI-GO-6	0.2439
5	PANI-GO-8	0.1694
6	PANI-GO-10	0.2083
7	PANI-DBSA	0.0450

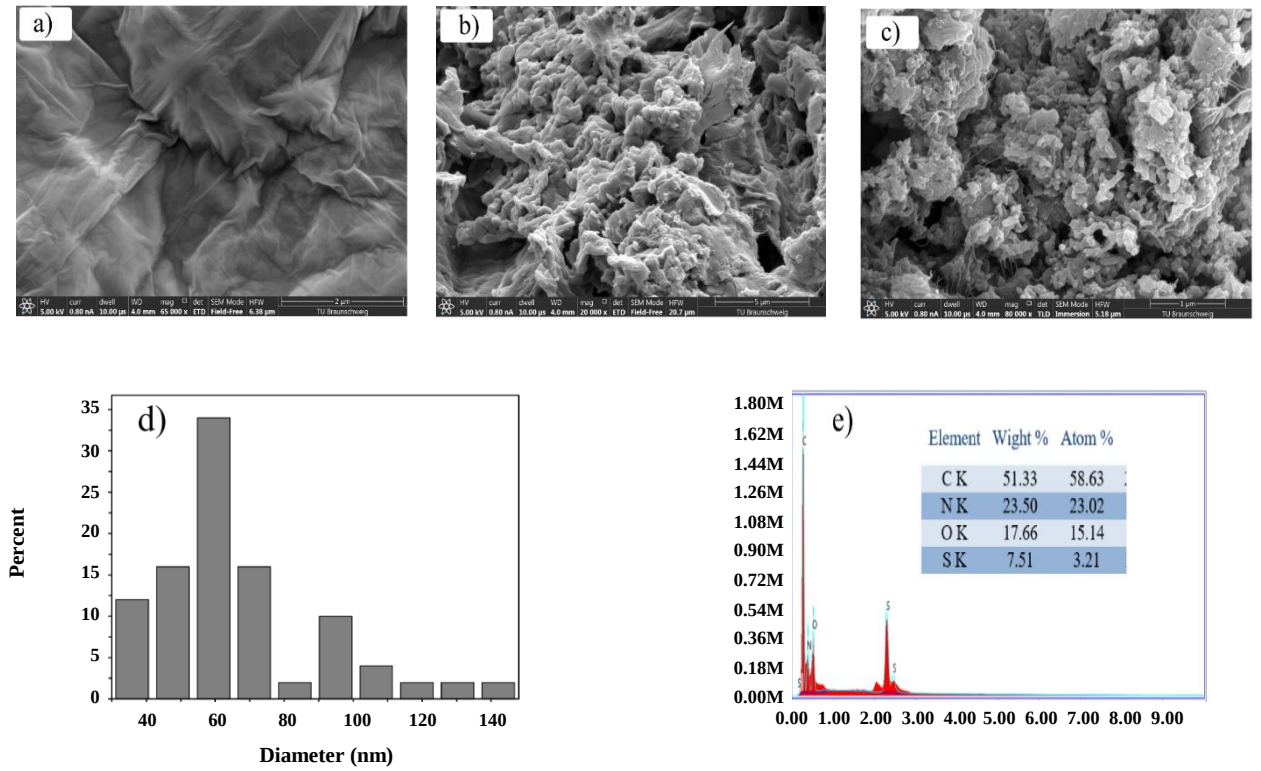

Fig. 3: (a) SEM images of GO; (b) PANI; (c) PANI-GO-6; (d) Histogram of particle size (PANI-GO-6); (e) EDX pattern for PANI-GO-6.

for this enhanced electrical conductivity could be illustrated on the basis of the generation of mutual conducting pathways among PANI and GO which create a bridge between these two components [22]. The crystallinity of PANI and composites of PANI with GO, greatly affect its electrical conductivity. Well-organized PANI structure, in emeraldine oxidation state and doped form, is the main reason for charge transfer inside PANI's chains. Higher electrical conductivity in PANI-GO composites might be due to the growth of PANI chains on the surface of highly ordered GO sheets [23]. These results are in accordance with XRD analysis, which contains very sharp peaks (highly crystalline structure) for PANI in PANI-GO composites.

However, the conductivity first increases, and then there is a slight decrease when the amount of GO was further increased. This might be due to an increase in the resistivity of the composites due to the poor conductivity of GO [24].

Thermogravimetry Analysis

A useful technique for determination of dopants and water content in the polymers is ThermoGravimetry

Analysis (TGA). Additionally, it is used to find out thermal degradation patterns, structural aspects, and thermal stability [1]. The mass loss profile is obtained from the mass loss step.

To test the thermal stability and check the behavior of GO, PANI, and PANI-GO at a higher temperature, TGA analysis was carried out (Fig. 4). As is clear from Fig. 4 (a), GO weight loss starts before 100 ºC, this might be due to removal of physically adsorbed water [25]. While up to 251 ºC temperature, its weight loss is 45% of total weight. This weight loss can be assigned to pyrolysis of the labile oxygen-containing functional groups that are present in GO [26].

From Fig. 4, PANI manifests three steps of decomposition. The decomposition prior to 260 ºC is mainly due to the deprivation of moisture content and dopant. PANI backbone begins to break down at a temperature above 260 ºC.

TGA plot for PANI-GO composites exhibits typical decomposition steps of PANI. The first step in weight loss is because of the elimination of moisture. The second weight-loss step is because of the elimination of dopant [27] However, PANI-GO exhibits a rapid mass loss around 300 ºC which might be due to the decomposition of oxygen-containing groups, such as –OH, –CO–, and –COOH [13].

In Fig. 4, it is clear that thermal stability for composites is shifted in direction of elevated temperature in comparison to PANI and GO. As complete decomposition of PANI occurs at 639 ºC while for PANI-GO-6 it is shifted to 825 ºC. This improved thermal stability of covalently-grafted composites cab is assigned to the covalent bonding among GO and PANI backbone [28]. Also, the covalent bonding results in a substantial π-π stacking force among the basal plane of GO and the PANI backbone [29]. Thus, from Fig. 4, the formation of composite and interaction among PANI and GO results in enhanced thermal stability when compared with pure PANI and GO.

Kinetic Analysis of TGA Data:

Significant kinetic parameters (pre-exponential factor, activation energy, order, and mechanism of a reaction) can be calculated by using TGA. Knowledge of these parameters is important for investigating thermal stability and hence the behavior of the materials at high temperatures [2]. Various mechanisms have evolved for the determination of kinetic variables of reactions that happen in the solid state. Generally, the kinetics of the condensed and heterogeneous phase reactions take place in the non-isothermal state and is evaluated by employing Eq. (3).

$$\beta\left(\frac{d\alpha}{dT}\right) = A f(\alpha) e^{-\frac{Ea}{RT}} \quad (3)$$

In the above equation, $f(\alpha)$ is the differential conversion function, α is the extent of transformation, T is the temperature, β is the linear heating rate, R is the gas constant, the pre-exponential factor is A and Ea is the activation energy.

The kinetic triplet (A, E, $f(\alpha)$) can be determined as differential, integral or other. In the present work, two well-liked methods are applied for evaluating kinetic parameters for the degradation of synthesized composites which assumes first-order kinetics.

Horowitz and Metzger Method

An equation was put forward by Horowitz and Metzger for the manipulation of pyrolysis parameters through analyzing TGA data. Based on this equation a plot of $ln[ln\{(Wo-Wf)/(Wt-Wf)\}]$ $ln[ln\{(Wo-Wf)/(Wt-Wf)\}]$ (double logarithm of the reciprocal of the reactant weight) versus temperature provide the activation energy of degradation. Equation (4) was put forward to evaluate first-order reaction kinetics [30, 31].

$$\ln\left[\ln\left(\frac{W_o - W_f}{W_t - W_f}\right)\right] = \frac{Ea\theta}{RT_s^2} \quad (4)$$

Whereas Wo is weight at the beginning of the experiment, Wt is the weight of the material at onward temperature, Wf is weight at the end, R is the general gas constant and θ is equal to T-Ts where Ts is the reference temperature which can be obtained from the following relation:

$$\frac{(W_t - W_f)}{(W_0 - W_f)} = \frac{1}{e} \quad (5)$$

Ts is the experimental temperature when W_t-W_f/W_o-W_f is equal to 0.368 for a first-order reaction [2].

Thus, Ea can be computed from the slope ($Ea \times 10^3 / RTs^2$) of a plot of the double logarithm of the reciprocal of the weight fraction of the reactant vs the corresponding temperature.

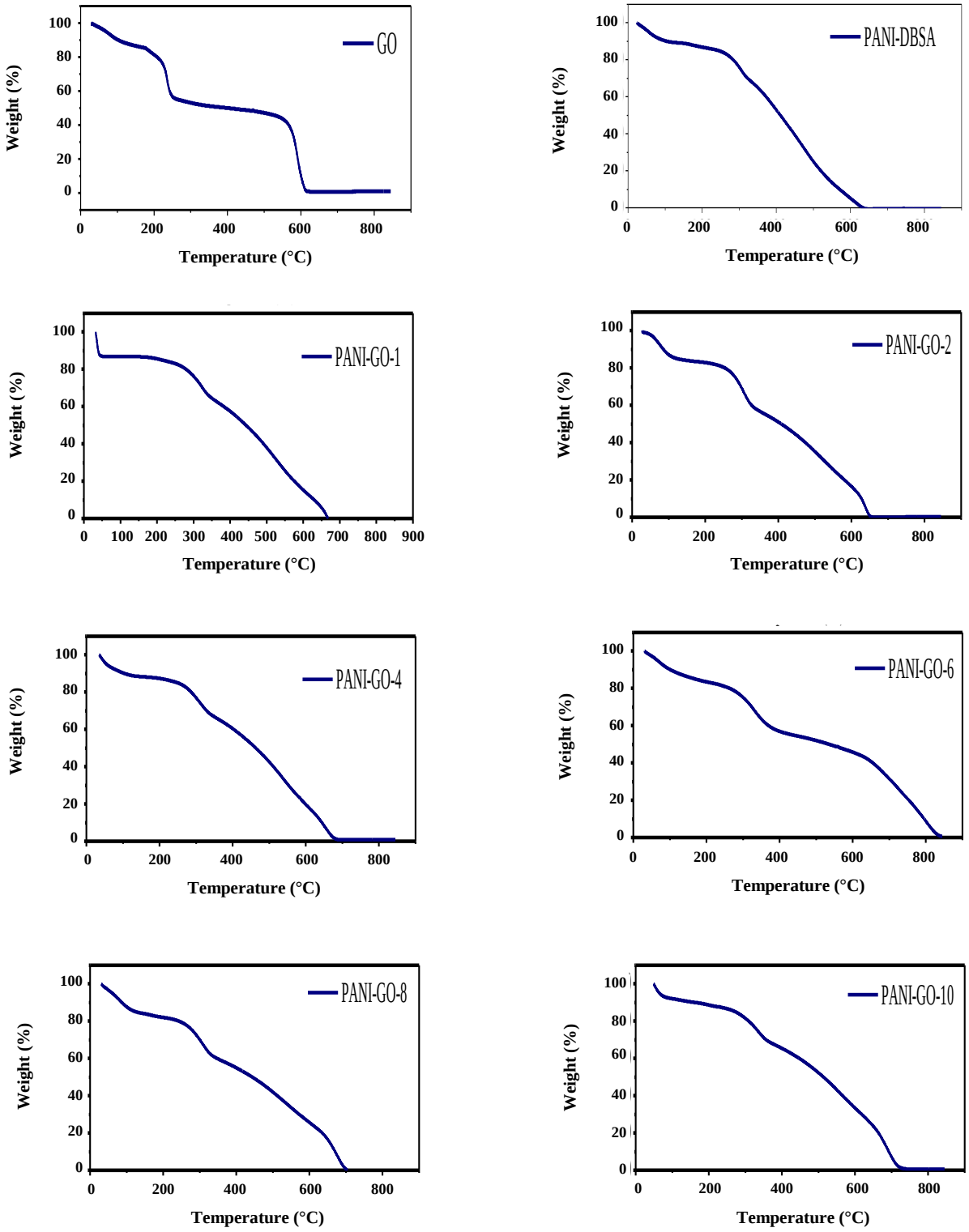

Fig. 4: TGA analysis of GO, PANI, and PANI-GO composites.

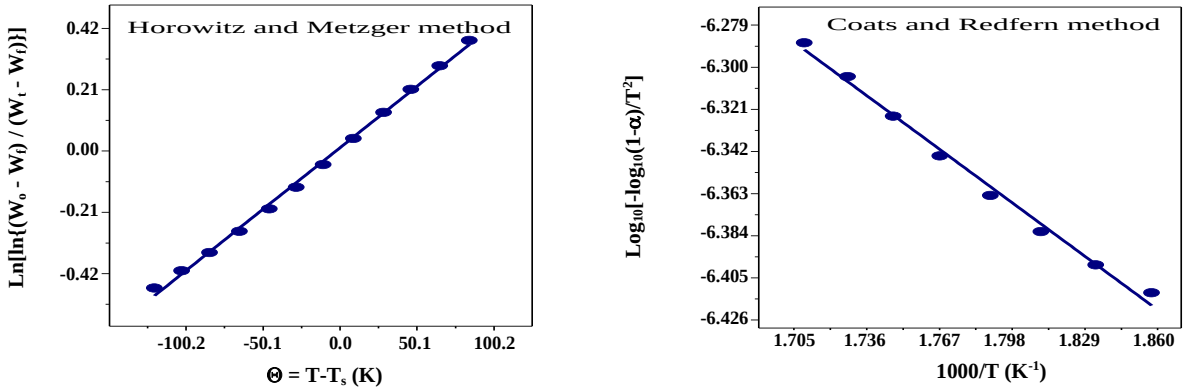

Fig. 5: Plots for calculating activation energy of PANI-GO-6.

Coats and Redfern Method

Coats and *Redfern* [2] derived an expression for determining the energy of activation that contained the order of reaction as an important parameter. The rate of disappearance of the reactant can be expressed as

$$\frac{d\alpha}{dt} = k(1-\alpha)^n \quad (6)$$

Where α is a fraction of reactant decomposition at time t, the order of reaction (n) and the rate constant (k) is given as:

$$k = A\exp\left(\frac{-Ea}{RT}\right) \quad (7)$$

A is the frequency factor, R is the universal gas constant and Ea is the activation energy of the reaction. For a linear heating rate of say a degree per minute

$$a = \left(\frac{dT}{dt}\right) \quad (8)$$

Combining Equation (6)-(8), rearranging and integrating:

$$\int_0^a \frac{d\alpha}{(1-\alpha)^n} = \left(\frac{A}{a}\right)\int_0^T \exp\left(\frac{-Ea}{RT}\right)dT \quad (9)$$

$$\log_{10}\left[\frac{1-(1-\alpha)^{1-n}}{T^2(1-n)}\right] = \left\{\log_{10}\left(\frac{AR}{aEa}\right)\left[1-\left(\frac{2R}{Ea}\right)\right]\right\} - \left(\frac{Ea}{2.3RT}\right) \quad (10)$$

For all values of n except n=1 in which case Eq. (9) after taking log becomes:

$$\log_{10}\left[\frac{1-(1-\alpha)}{T^2}\right] = \left\{\log_{10}\left(\frac{AR}{aEa}\right)\left[1-\left(\frac{2R}{Ea}\right)\right]\right\} - \left(\frac{Ea}{2.3RT}\right) \quad (11)$$

Thus a plot of either $log_{10}\{1-(1-\alpha)^{1-n}/[T^2(1-n)]\}$ against T^{-1} followed bt the integration gives rise to the expression for $n=1$. When $n=1$ i.e. first-order reaction, $log_{10}[-log_{10}(1-\alpha)/T^2]$ against $1000/T$ gives plot of straight line with a slop ($Ea / 2.303R$), for which Ea can be calculated [32, 33].

Fig. 5 and Fig. S5-10, show graphs obtained through TGA data. The activation energies were calculated by using Horowitz and Metzger and Coats and Redfern, which are 14.34-29.87 kJ/mol and 11.61-16.47kJ/mol, respectively (Table 3).

From Table 3, it is clear that activation energy for degradation of PANI-GO-6 calculated through both methods is the highest among all samples. For Horowitz and Metzger method its value is 29.87 kJ/mol while for the Coats and Redfern method is 16.47 kJ/mol. These results are consistent with TGA plots depicted in Fig. 4, that PANI-GO-6 is thermally the most stable among all samples. It might be due to better interaction among PANI and GO [29].

Chan et al., Method

To further get information about the degradation kinetics Chan et al. method was used to calculate activation energy and pre-exponential factor for PANI-GO-6 (Fig. 6). *Chan et al*. used the Arrhenius plot for the calculation of activation energy by assuming the first-order reaction

Table 3: Activation energy calculated using Horowitz and Metzger and Coats and Redfern method.

S. No	Sample name	Activation Energy (kJ/mol)	
		Horowitz and Metzger method	Coats and Redfern method
1	PANI	14.34	11.61
2	PANI-GO-1	22.8	11.86
3	PANI-GO-2	22.6	12.24
4	PANI-GO-4	27.66	12.24
5	PANI-GO-6	29.87	16.47
6	PANI-GO-8	24.17	11.88
7	PANI-GO-10	29.83	14.25

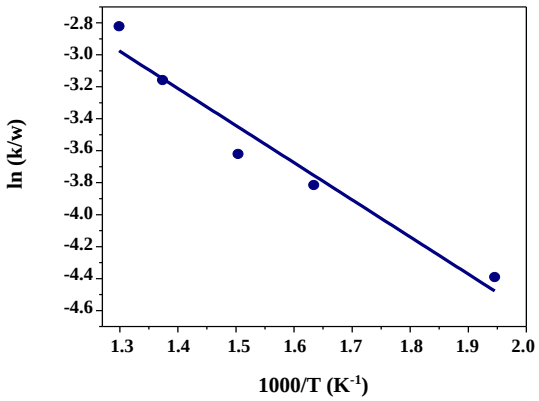

Fig. 6: Chan et al. method for PANI-GO-6.

kinetics [34]. Arrhenius plot of (*ln k/w*) vs *1/T* gives the slope *(-Ea/R*). From the slope of this plot activation energy of degradation, the material can be calculated whereas *k* is the rate of percent weight loss; *w* is the corresponding percent weight of the remaining material. The activation energy "*Ea*" for PANI-GO-6, was found to be 19.28 kJ/mol. From the intercept, the value of the pre-exponential factor (*lnA*) is 0.042.

The results show that when experimental data of TGA was analyzed by different methods of analysis, the calculated values for kinetic parameters were not similar. This phenomenon was explained by Brown [35]. Detail study was carried out regarding the calculation of *Ea* using non-isothermal data. The authors proposed that variation in the values is because of the way in which the integral method has been derived. These equations have been developed by assuming that activation parameters are independent of α (degree of conversion).

CONCLUSIONS

It can be concluded that changing composition has a remarkable effect on the thermal stability of polymeric composites. To get a composite with the best possible properties, effective interaction of these components is necessary. The values of activation energy for degradation calculated using different methods are different. The activation energies calculated by using the Coats and Redfern method, (e.g., for PANI-GO-6 is 16.47 kJ/mol) are less than the *Ea* values acquired by Horowitz and Metzger method (e.g., for PANI-GO-6 is 29.87 kJ/mol). While using *Chan et al*., method activation energy was found to be 19.28 kJ/mol for PANI-GO-6. These variations among the activation energies can be due to different approximations of the temperature integral. These values may not be the most accurate, but an approximate range of the parameters can be acquired. The data of activation energy calculated by each specific method can give an idea of the relative thermal stabilities of the different polymers. Different parameters in differential equations are the reason for different values obtained from different methods. However, the general trend in the values of activation energy of degradation was the same. Among all samples, PANI-GO composite with 6% GO showed the highest thermal stability up to 825 °C and the highest activation energy for degradation obtained from all methods.

Received : Jul. 11, 2020 ; Accepted : Dec. 7, 2020

REFERENCES

[1] Gul H., Shah A.U.A., Gul S., Arjomandi J., Bilal S., Study on the Thermal Decomposition Kinetics and Calculation of Activation Energy of Degradation of Poly (o-toluidine) Using Thermogravimetric Analysis, *Iran. J. Chem. Chem. Eng. (IJCCE)*, **37**: 193-204 (2018)

[2] Abthagir P.S., Saraswathi R., Sivakolunthu S., Aging and Thermal Degradation of Poly (N-methylaniline), *Thermochim. Acta*, **411**: 109-123 (2004)

[3] Cai J., Bi L., Precision of the Coats and Redfern Method for the Determination of the Activation Energy without Neglecting the Low-Temperature End of the Temperature Integral, *Energy Fuels*, **22**: 2172-2174 (2008)

[4] Órfão J.J., Review and Evaluation of the Approximations to the Temperature Integral, *AlChE J.*, **53**: 2905-2915 (2007)

[5] Ebrahimi-Kahrizsangi R., Abbasi M.H., Evaluation of Reliability of Coats-Redfern Method for Kinetic Analysis of Non-Isothermal TGA, *Trans. Nonferrous Met. Soc. China*, **18**: 217-221 (2008)

[6] Regnier N., Guibe C., Methodology for Multistage Degradation of Polyimide Polymer, *Polym. Degrad. Stab.* **55**: 165-172 (1997)

[7] Jafari Y., Ghoreishi S.M., Shabani-Nooshabadi, M., Electrosynthesis, Characterization and Corrosion Inhibition Study of DBSA-Doped Polyaniline Coating on 310 Stainless Steel, *Iran. J. Chem. Chem. Eng. (IJCCE)*, **36**: 23-32 (2017).

[8] Valiollahi M.H., Abbasian, M., Pakzad, M., Synthesis and Characterization of Polyaniline-Polystyrene-Chitosan/Zinc Oxide Hybrid Nanocomposite, *Iran. J. Chem. Chem. Eng. (IJCCE)*, **38**: 55-64 (2019).

[9] Tong Z., Yang Y., Wang J., Zhao J., Su B.L., Li Y., Layered Polyaniline/Graphene Film from Sandwich-Structured Polyaniline/Graphene/Polyaniline Nanosheets for High-Performance Pseudosupercapacitors, *J. Mater. Chem. A*, **2**: 4642-4651 (2014)

[10] Gul H., Shah A.U.A., Krewer U., Bilal S., Study on Direct Synthesis of Energy Efficient Multifunctional Polyaniline–Graphene Oxide Nanocomposite and Its Application in Aqueous Symmetric Supercapacitor Devices, *Nanomaterials*, **10**: 118 (2020

[11] Vargas L.R., Poli A.K., Dutra R.D.C.L., Souza C.B.D., Baldan M.R., Gonçalves E.S., Formation of Composite Polyaniline and Graphene Oxide by Physical Mixture Method, *J. Aerosp. Technol. Manag*, **9**: 29-38 (2017)

[12] Zhao Y., Tang G.S., Yu Z.Z., Qi J.S., The Effect of Graphite Oxide on the Thermoelectric Properties of Polyaniline, *Carbon*, **50**: 3064-3073 (2012)

[13] Gul H., Fabrication of Energy-Efficient Ultracapacitive Electrodes Based on Conducting Polyaniline-Graphene Oxide Composites, (*Doctoral dissertation, University of Peshawar, Peshawar*), (2019).

[14] Ma K., Wang R., Jiao T., Zhou J., Zhang L., Li J., Bai Z., Peng, Q., Preparation and Aggregate State Regulation of Co-Assembly Graphene Oxide-Porphyrin Composite Langmuir Films *via* Surface-Modified Graphene Oxide Sheets, *Colloid Surface A*, **584**: 124023 (2020).

[15] Gul H., Shah A.U.H.A., Bilal, S., Achieving Ultrahigh Cycling Stability and Extended Potential Window for Supercapacitors Through Asymmetric Combination of Conductive Polymer Nanocomposite and Activated Carbon, *Polymers*, **11**: 1678 (2019).

[16] Liu L., Zhou W., Chen Y., Jiao S., Huang P., Pressure-Assisted Synthesis of a Polyaniline–Graphite Oxide (PANI–GO) Hybrid and Its Friction Reducing Behavior in Liquid Paraffin (LP), *New J. Chem.*, **42:** 936-942 (2018)

[17] Afzali M., Mostafavi A., Shamspur T., Square Wave Voltammetric Determination of Anticancer Drug Flutamide Using Carbon Paste Electrode Modified by CuO/GO/PANI Nanocomposite, *Arabian J. Chem.*, (in press) (2018)

[18] Javed M.S., Dai S., Wang M., Guo D., Chen L., Wang X., Hu C., Xi Y., High Performance Solid State Flexible Supercapacitor Based on Molybdenum Sulfide Hierarchical Nanospheres, *J. Power Sources*, **285:** 63-69 (2015)

[19] Gul H., Shah A.U.A., Bilal S., Fabrication of Eco-Friendly Solid-State Symmetric Ultracapacitor Device Based on Co-Doped PANI/GO Composite, *Polymers*, **11:** 1315 (2019)

[20] Purkait T., Singh G., Kumar D., Singh M., Dey R.S., High-Performance Flexible Supercapacitors Based on Electrochemically Tailored Three-Dimensional Reduced Graphene Oxide Networks, *Sci. Rep.*, **8:** 640 (1-13) (2018)

[21] Fan Y.J., Yu P.T., Liang F., Li X., Li H.Y., Liu L., Cao J.W., Zhao X.J., Wang Z.L., Zhu, G., Highly Conductive, Stretchable, and Breathable Epidermal Electrode Based on Hierarchically Interactive Nano-Network, *Nanoscale*, **12**: 16053-16062 (2020).

[22] Ramezanzadeh B., Moghadam M.M., Shohani N., Mahdavian M., Effects of Highly Crystalline and Conductive Polyaniline/Graphene Oxide Composites on the Corrosion Protection Performance of a Zinc-Rich Epoxy Coating, *Chem. Eng. J.*, **320:** 363-375 (2017)

[23] Moshayedi H.R., Rabiee M., Rabiee N., Graphene Oxide/Polyaniline-Based Multi Nano Sensor for Simultaneous Detection of Carbon Dioxide, Methane, Ethanol and Ammonia Gases, *Iran. J. Chem. Chem. Eng (IJCCE).*, **39**: 55-64 (2020)

[24] Wang H., Hao Q., Yang X., Lu L., Wang X., Effect of Graphene Oxide on the Properties of its Composite with Polyaniline, *ACS Appl. Mater. Interfaces*, **2:** 821-828 (2010)

[25] Li Z.F., Zhang H., Liu Q., Liu Y., Stanciu L., Xie J., Covalently-Grafted Polyaniline on Graphene Oxide Sheets for High Performance Electrochemical Supercapacitors, *Carbon*, **71:** 257-267 (2014)

[26] Nguyen T. X., Nguyen M.T., Nguyen H. V., Hoang H.V., Synthesis of Graphene Titanium Dioxide Composites as Photocatalytic Materials for Degradation of Moderacid Black, *Asian J. Chem*., **28**: 1297-1303 (2016)

[27] Bilal S., Gul H., Gul S., Shah A.U.A., One Pot Synthesis of Highly Thermally Stable Poly (2-Methylaniline) for Corrosion Protection of Stainless Steel, *Iran J Sci Technol Trans Sci.*, **42:** 1915-1922 (2018)

[28] Tang X.Z., Li W., Yu Z.Z., Rafiee M.A., Rafiee J., Yavari F., Koratkar N., Enhanced Thermal Stability In Graphene Oxide Covalently Functionalized with 2-amino-4, 6-didodecylamino-1, 3, 5-triazine, *Carbon*, **49**: 1258-1265 (2011)

[29] Luo J., Jiang S., Wu Y., Chen M., Liu X., Synthesis of Stable Aqueous Dispersion of Graphene/Polyaniline Composite Mediated by Polystyrene Sulfonic Acid, *J. Polym. Sci., Part A: Polym. Chem.*, **50:** 4888-4894 (2011)

[30] Yang G., Heo Y.J., Park S.J., Effect of Morphology of Calcium Carbonate on Toughness Behavior and Thermal Stability of Epoxy-Based Composites, *Processes*, **7**: 178 (2019)

[31] Riaz S., Park S.J., Thermal and Mechanical Interfacial Behaviors of Graphene Oxide-Reinforced Epoxy Composites Cured by Thermal Latent Catalyst, *Materials*, **12:** 1354 (2019)

[32] Boukaous N., Abdelouahed L., Chikhi M., Meniai A.H., Mohabeer C., Bechara T., Combustion of Flax Shives, Beech Wood, Pure Woody Pseudo-Components and Their Chars: A Thermal and Kinetic Study, *Energies*, **11:** 2146 (2018)

[33] Chen S., Xiao M., Sun L., Meng Y., Study on Thermal Decomposition Behaviors of Terpolymers of Carbon Dioxide, Propylene Oxide, and Cyclohexene Oxide, *Int. J. Mol. Sci.*, **19:** 3723(2018)

[34] Chan H.S.O., Ho P.K.H., Khor E., Tan M.M., Tan K.L., Tan B.T.G., Lim Y.K., Preparation of Polyanilines Doped in Mixed Protonic Acids: Their Characterization by X-Ray Photoelectron Spectroscopy and Thermogravimetry, *Synth. Met.*, **31**: 95-108 (1989)

[35] Brown M., Steps in a Minefield: Some Kinetic Aspects of Thermal Analysis, *J. Therm. Anal. Calorim.*, **49**: 17-32 (1997)